

Article

Capillary Electrophoresis as Analysis Technique for Battery Electrolytes: (i) Monitoring Stability of Anions in Ionic Liquids and (ii) Determination of Organophosphate-Based Decomposition Products in LiPF₆-Based Lithium Ion Battery Electrolytes

Marcelina Pyschik ¹, Martin Winter ^{1,2} and Sascha Nowak ^{1,*} 

¹ MEET Battery Research Center, Institute of Physical Chemistry, University of Muenster, Corrensstraße 46, 48149 Muenster, Germany; marcelina.pyschik@uni-muenster.de

² Forschungszentrum Juelich GmbH, Helmholtz Institute Muenster, IEK-12, Corrensstraße 46, 48149 Muenster, Germany; martin.winter@uni-muenster.de

* Correspondence: sascha.nowak@uni-muenster.de; Tel.: 49-251-833-6735

Received: 1 August 2017; Accepted: 24 August 2017; Published: 5 September 2017

Abstract: In this work, a method for capillary electrophoresis (CE) hyphenated to a high-resolution mass spectrometer was presented for monitoring the stability of anions in ionic liquids (ILs) and in commonly used lithium ion battery (LIB) electrolytes. The investigated ILs were 1-methyl-1-propylpyrrolidinium bis(trifluoromethanesulfonyl)imide (PYR₁₃TFSI) and 1-methyl-1-propylpyrrolidinium bis(fluorosulfonyl)imide (PYR₁₃FSI). The method development was conducted by adjusting the following parameters: buffer compositions, buffer concentrations, and the pH value. Also the temperature and the voltage applied on the capillary were optimized. The ILs were aged at room temperature and at 60 °C for 16 months each. At both temperatures, no anionic decomposition products of the FSI[−] and TFSI[−] anions were detected. Accordingly, the FSI[−] and TFSI[−] anions were thermally stable at these conditions. This method was also applied for the investigation of LIB electrolyte samples, which were aged at 60 °C for one month. The LP30 (50/50 wt. % dimethyl carbonate/ethylene carbonate and 1 M lithium hexafluorophosphate) electrolyte was mixed with the additive 1,3-propane sultone (PS) and with one of the following organophosphates (OP): dimethyl phosphate (DMP), diethyl phosphate (DEP), and triethyl phosphate (TEP), to investigate the influence of these compounds on the formation of OPs.

Keywords: ionic liquids; capillary electrophoresis; quadrupole time-of-flight mass spectrometer; thermal stability study; lithium ion battery electrolyte

1. Introduction

Ionic liquids (ILs) are molten salts that are liquids below 100 °C. They are used in different application fields as separation aid for complex analytes, as sample preparation methods for chromatographic analysis, or as electrolyte components in lithium ion batteries (LIBs) [1–6]. For the use of IL-based electrolytes for LIBs, high thermal stability as well as flame retardant performance and negligible vapor pressure are considered beneficial [7]. According to the literature, the most commonly used anion is bis(trifluoromethanesulfonyl)imide (TFSI). However, one disadvantage is that it supports anodic dissolution of the typically used aluminum current collector [8–10], which is often erroneously called “corrosion” [11,12]. In contrast, the advantages of the TFSI[−] anion are its high thermal stability and its suitable physicochemical properties in electrolyte solutions. Most of the thermal stability studies so far were carried out by thermogravimetric analysis (TGA), with or without hyphenation to a mass

spectrometer (MS) [13–21]. These investigations were performed at temperatures above 350 °C. At such high temperatures, the ILs decompose. Furthermore, in several studies, the thermal stability of the ILs was investigated by spectroscopic methods [22–26]. In these techniques, all components are analyzed simultaneously. Therefore, low concentrations of decomposition products can overlap with the signal of the main compounds and thus may not be properly analyzed. Chromatographic methods hyphenated to suitable detectors can achieve the separation of impurities or decomposition products from the ILs. Hao et al. developed a method to analyze halide impurities in ILs using ion chromatography (IC) [27]. In addition, Villagrán et al. quantified chloride using IC and showed that chloride ions change the density and viscosity of the ILs [28]. Pyschik et al. investigated different TFSI[−] anions and bis(fluorosulfonyl)imide based (FSI) ILs mixed with lithium hexafluorophosphate (LiPF₆), lithium perchlorate or lithium TFSI, using IC and capillary electrophoresis (CE) hyphenated to a mass spectrometer, as well as possible decomposition routes for ILs-based cations [29–32]. They reported that FSI[−] degraded when aged together with hexafluorophosphate or perchlorate anions, whereas TFSI[−] did not show any aging. [29] Standard LIB electrolytes consist of LiPF₆ in liquid organic carbonate solvents [33]. The thermal stability of LiPF₆ in mixtures with these carbonates is much lower than the thermal stability of the pure LiPF₆ salt. The pure salt is stable up to 194 °C [34], whereas in mixtures of LiPF₆ and carbonates, the hydrolysis products and the decomposition products from the reaction of the lithium salt and the carbonates are formed above 60 °C or even at lower temperatures [35,36]. During the degradation reactions, various non-ionic and ionic organophosphates (OPs) as decomposition products were reported [35,37–40], which affect the electrochemical cell performance [37,38,41–49]. In this work, a capillary electrophoresis method is introduced for the investigation of anions in ILs and organophosphates (OPs) in lithium ion battery (LIB) electrolytes. The ILs 1-methyl-1-propylpyrrolidinium bis(trifluoromethanesulfonyl)imide (PYR₁₃TFSI) and 1-methyl-1-propylpyrrolidinium bis(fluorosulfonyl)imide (PYR₁₃FSI) were aged at room temperature and at 60 °C. Additionally, this CE method was applied to investigate fresh and aged electrolyte samples. Each sample was mixed with the electrolyte additive 1,3-propane sultone (PS) and either dimethyl phosphate (DMP), diethyl phosphate (DEP), or triethyl phosphate (TEP), to investigate the influence of these phosphates on the formation of other OPs. For reference measurements, the electrolyte was aged without electrolyte additive and without OP.

2. Materials and Methods

For the detection of the anionic decomposition products of PYR₁₃TFSI and PYR₁₃FSI, the CE 7100 from Agilent Technologies (Santa Clara, CA, USA) hyphenated to the 6530 Accurate Mass Quadrupole Time of Flight Mass Analyzer (Q-TOF) with an electrospray ionization (ESI) coaxial sheath liquid interface was used. PYR₁₃FSI and PYR₁₃TFSI were synthesized according to the procedure published by Appetecchi et al. [50]. The electrolyte SelectiLyte LP30 (50/50 wt. % DMC/EC and 1 M LiPF₆ (battery grade purity) were ordered from BASF (Ludwigshafen, Germany) (max. 20 ppm water). PS (99% purity), dimethyl phosphate (DMP), diethyl phosphate (DEP, 99%), and triethyl phosphate (TEP, 99.8%) were obtained from Sigma Aldrich (Steinheim, Germany). The sheath liquid consisted of 5 mM ammonium hydroxide obtained from Merck KGaA (Darmstadt, Germany), and was diluted in 50.0% methanol (HPLC grade) obtained from Merck KGaA (Darmstadt, Germany) and 50.0 vol. % Milli-Q water (*v/v*), produced by an in-house Millipore filter system (18.2 MΩ cm, TOC < 3 ppb, Milli-Q Advantage A10, Millipore GmbH, Schwalbach, Germany). The sheath liquid was pumped by an isocratic pump 1260 (Agilent Technologies, Santa Clara, CA, USA). The software MassHunter Acquisition B.05.01 software from Agilent Technologies (Santa Clara, CA, USA) was used to control the hyphenation between the CE and the Q-TOF system and for the interpretation of the data MassHunter Qualitative B.07.00 software was used. The sheath liquid was delivered with a flow rate of 8 μL/min. The standard bare fused silica capillary was obtained from Polymicro (Phoenix, AZ, USA) and had an inner diameter (i.d.) of 50 μm and a total length of 100 cm. The capillary was preconditioned by rinsing with the buffer for 10 min. The buffer consisted of 10 mM ammonium acetate purchased from Acros Organics (98.0%, Geel, Belgium). The pH-value of 10.34 was adjusted by ammonia. The system

was rinsed with buffer for 10 min between the measurement steps to protect the capillary from contamination of the previous run. The applied ESI-Q-TOF-MS parameters, which were optimized for a m/z range of 50–500, were as follows: for ESI(-) mode, the capillary voltage was 3000 V, dry gas was set up to 8 L/min, and nebulizer pressure to 10 psi with a dry temperature of 250 °C. The applied voltage on the capillary was 30 kV. The samples were injected hydrodynamically in the CE by applying a pressure of 50 mbar for 2 s. Afterwards, the buffer was injected for 2 s at the same conditions. The ILs were stored at room temperature and at 60 °C to investigate the decomposition products of the anions. For the measurements, the aged ILs were diluted in a ratio of 1:500 with the buffer and 20.0 vol. % acetonitrile. Additionally, the fresh and aged LP30 electrolyte was investigated. The aging of the LP30 electrolyte was carried out at 60 °C for one month. For all measurements, the electrolyte samples were diluted in a ratio of 1:500 with the buffer solution.

3. Results and Discussion

3.1. Method Development for the Detection of Anions in Ionic Liquids

In order to analyze the anions in ILs, several CE conditions such as buffer composition, pH value, temperature, and applied capillary voltage were optimized. Since the CE was hyphenated to the ESI-Q-TOF-MS, it was essential to use a volatile buffer for the separation of the anions. Two volatile buffers were tested for the detection of the TFSI[−] anion, 40.0 mM ammonium formate buffer (A) and 50.0 mM ammonium acetate buffer (B) (Figure 1). Both peaks A and B, had a m/z ratio 279.9173 corresponding to the anion TFSI[−]. The concentrations and sample preparations of these two samples were identical. The peak intensity using the ammonium acetate buffer was higher than using the ammonium formate buffer, by a factor of 10. As a result, further optimization measurements were carried out using the ammonium acetate buffer.

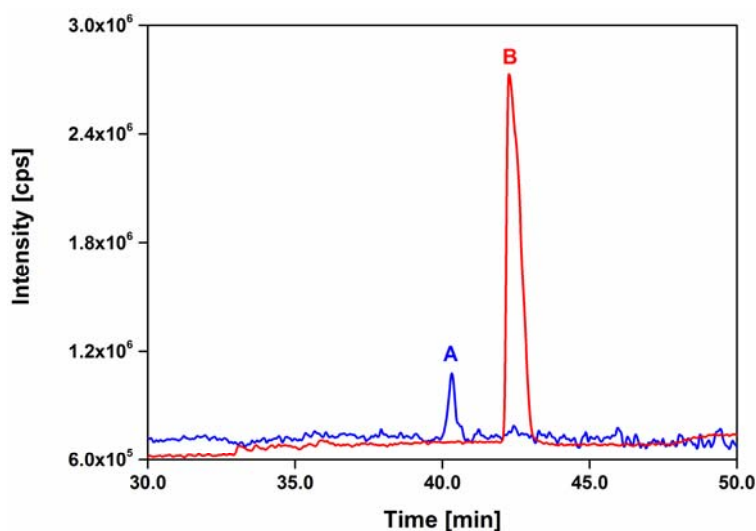


Figure 1. Electropherogram of bis(trifluoromethanesulfonyl)imide (TFSI[−]) with the buffers A (40.0 mM ammonium formate buffer) and B (50.0 mM ammonium acetate buffer).

Another important parameter of the buffer solution is the pH value. The pH value affects the electro-osmotic flow (EOF), which has an influence on ion separation. To investigate this effect, ammonium acetate (25.0 mM) was adjusted to the pH values of 10.34, 10.08, and 9.41, with an ammonia solution (25.0%). In Figure 2 A, the correlation between the migration time of TFSI[−] and different pH-values is presented. Increased pH values led to a decrease in the migration time and a sharper peak form. The highest intensity of TFSI[−] was observed at the highest pH-value (10.34). The differences

concerning the migration time and peak form were not as significant between pH 10.34 and 10.08, as between pH 9.41 and 10.08. Therefore, the pH value was adjusted to a value of 10.34.

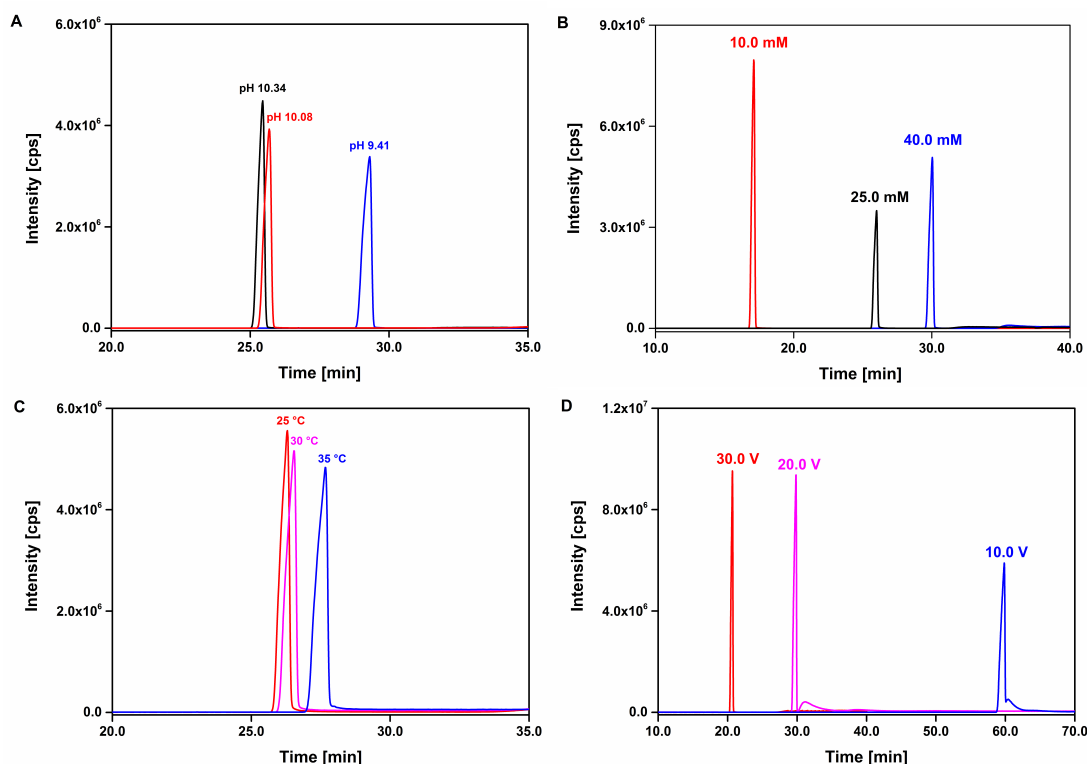


Figure 2. Electropherograms showing the TFSI[−] peak using an acetate buffer during method development: (A) measured at different pH values; (B) measured with different concentrations of the acetate buffer; (C) measured at different temperatures and (D) measured under different applied voltages.

For the investigation of the effect of the buffer concentration on the migration time of the TFSI[−] anion, ammonium acetate buffers with the concentration of 10.0 mM, 25.0 mM and 40.0 mM were used (Figure 2B). The pH values of the three ammonium acetate buffers were adjusted to 10.34. The migration time of TFSI[−] was shorter with decreasing concentrations of the buffer solution. With a buffer solution of 10.0 mM, the shortest migration time of approx. 17.0 min of the TFSI[−] was achieved. In addition, the highest intensity and sharpest signal were obtained with this ammonium acetate buffer (10.0 mM). Therefore, the applied concentration of the ammonium acetate buffer for the detection of the TFSI[−] was 10.0 mM. For additional optimization of the CE method, the influence of temperature on the TFSI[−] peak was investigated (Figure 2C). For these investigations, the ammonium acetate buffer (concentration: 10.0 mM, pH: 10.34) was used at 25 °C, at 30 °C and at 35 °C. From this electropherogram (Figure 2C), it is obvious that a higher temperature resulted in a shorter migration time of the anion TFSI[−] when using the same buffer conditions. However, a temperature of 25 °C led to the sharpest peak with the highest intensity. The influence of the capillary voltage on the TFSI[−] anion can be observed in Figure 2D. For these investigations, the 10.0 mM ammonium acetate buffer with the pH-value of 10.3 at 25 °C was used. In the electropherogram (Figure 2D), it can be observed that a higher voltage resulted in shorter migration times of the anion. At lower voltages (20.0 kV and 10.0 kV), the TFSI[−] peak showed a shoulder. As a result, the best choice for the measurements was using a voltage of 30.0 kV. As a conclusion, the best results for the detection of the anions in ILs were obtained with 10.0 mM ammonium acetate buffer and a pH-value of 10.34. The following measurements were carried out at 25 °C and at a voltage of 30.0 kV.

3.2. Monitoring the Anionic Stability in Ionic Liquids

In Figure 3A, there was only one peak with a migration time of 20.1 min. This peak revealed an m/z ratio of 279.9173, which could be assigned to the anion TFSI[−]. The inset figure in Figure 3A shows the fresh TFSI[−] sample. The calculated m/z ratio of TFSI[−] was 279.9178 and the measured m/z ratio was 279.9173. The deviation was lower than 2 ppm. The same result was obtained for the samples aged at room temperature and at 60 °C. In conclusion, the temperature had no influence on the decomposition of the anion.

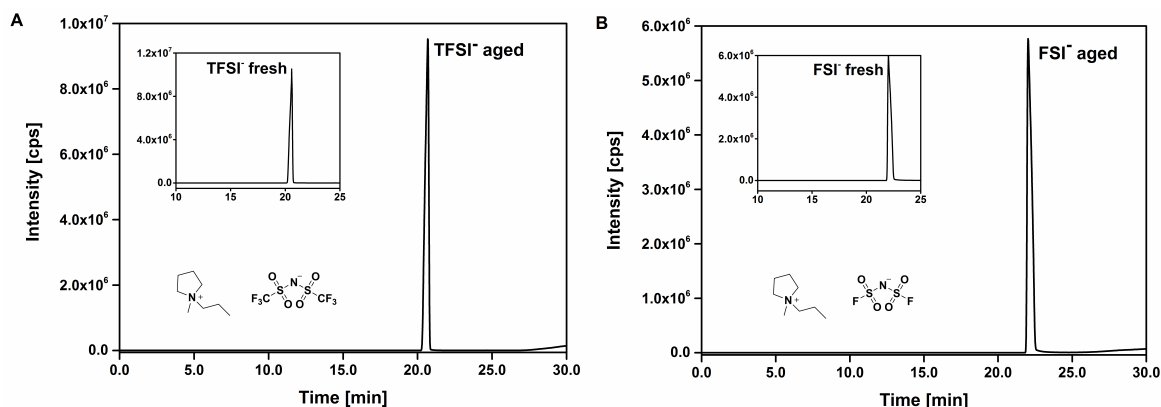


Figure 3. Electropherograms of the detected m/z ratio 279.9173 of the fresh and aged TFSI[−] sample (A) and of the detected m/z ratio 179.9238 of the fresh and aged FSI[−] sample (B).

In Figure 3B, one peak at a migration time of 22.5 min and a m/z ratio of 179.9238 was detected. In Figure 3B, the inserted figure shows the measurement of the fresh sample. The calculated m/z ratio of the FSI[−] was 179.9242. Accordingly, the deviation was 2.38 ppm. This peak was attributed to the FSI[−] anion aged at 60 °C. The same m/z ratios were also detected for the samples aged at room temperature. Overall, no decomposition products were observed. These results confirmed the stability study by Pyschik et al. in which the ILs were investigated by the hyphenation of ion chromatography and mass spectrometer [29]. Decomposition products were only detected for the FSI[−] anion mixed with the conductive salt lithium hexafluorophosphate or lithium perchlorate. No decomposition product of the TFSI[−] anion were observed [29]. Since no internal standard was used during the measurements, it was not possible to note changes in the areas.

3.3. Application for the Investigation of Decomposition Products in a LiPF₆-based Electrolyte

The electrolyte was aged at 60 °C for one month mixed with PS and with one of the following OPs: DMP, DEP and TEP. PS is a commonly used electrolyte additive in LIB electrolytes. DMP, DEP and TEP are possible decomposition products from the reaction of the lithium salt with the carbonates and are also used as flame retardants in LIB electrolytes [51]. As reference sample, the electrolyte was also aged without additive and without OPs. In Figure 4, the electropherogram of the reference sample is shown. Beside the detected m/z ratio of PF₆[−] (1), the decomposition product (2) with the m/z ratio of 122.9853 was determined at 12.6 minutes (see inset). In Table 1, all calculated and measured m/z ratios as well as the deviations and the related structures of the formed decomposition products mentioned in this part are given. Most of the deviations were in the range of 3 ppm. The combination of temperature and short storage time showed a slight aging of the electrolyte.

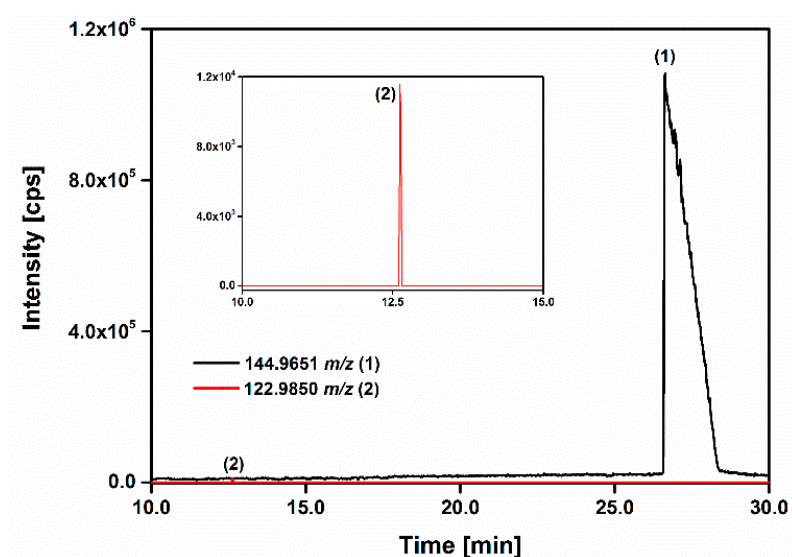
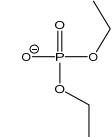
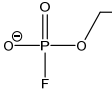


Figure 4. Electropherogram of the aged reference electrolyte sample.

Table 1. Proposed structures for the calculated and measured m/z ratios together with the deviation in ppm in the aged electrolyte samples.

Structure	Compound	Number	Calculated m/z Ratio	Measured m/z Ratio	Deviation (ppm)
<chem>[O-]P(=O)(F)(F)F</chem>	Hexafluoro phosphate	(1)	144.9642	144.9651	+6.20
<chem>[O-]P(=O)(OCCO)OCCO</chem>	Ethylene phosphate	(2)	122.9853	122.9850	−2.18
<chem>[O-]P(=O)(OCCO)OCCO</chem>	Hydroxy ethyl phosphate	(3)	185.0220	185.0218	−1.34
<chem>[O-]P(=O)(OCCO)OCCO</chem>	Ethoxyethyl ethyl phosphate	(4)	197.0584	197.0584	−0.17
<chem>[O-]P(=O)(OCCO)OCCO</chem>	Methoxyethyl methyl phosphate	(5)	169.0271	169.0277	+3.35
<chem>[O-]P(=O)(OCCO)OCCO</chem>	Methoxyethyl fluoro phosphate	(6)	157.0071	157.0069	−1.57
<chem>[O-]P(=O)(F)OC</chem>	Methyl fluoro phosphate	(7)	112.9809	112.9806	−2.94
<chem>[O-]P(=O)(F)OCCO</chem>	2-((fluoro (2-(phosphonooxy)ethoxy) phosphoryl) oxy) ethanolate	(8)	266.9840	266.9833	−2.78

Table 1. Cont.

Structure	Compound	Number	Calculated m/z Ratio	Measured m/z Ratio	Deviation (ppm)
	Diethyl phosphate	(9)	153.0322	153.0324	+1.18
	Ethyl fluoro phosphate	(10)	126.9966	126.9960	−4.59

In Figure 5, the electropherogram of the detected m/z ratios in the aged electrolyte sample with DMP and PS is shown. For a better overview, the peak of PF_6^- is not shown in the electropherogram. It is interesting that no m/z ratio of DMP was detected in the aged sample. Accordingly, DMP reacted completely to other decomposition products from the electrolyte mixture. The following OPs were determined in the aged sample: (2) 122.9850 m/z (3) 185.0218 m/z , (4) 197.0584 m/z , (5) 169.0277 m/z , (6) 157.0069 m/z , (7) 112.9806 m/z , and (8) 266.9833 m/z . Kraft and Weber et al. investigated this electrolyte by IC/ESI-MS and gas chromatography (GC)-MS and described the formation of several OPs in aged electrolytes [37,41,43–46]. In the electropherogram (Figure 5), some of the reported m/z ratios were detected. The advantage of the applied CE method is the baseline separation of the OPs without using a non-commercially available two-dimensional setup [46]. The two-dimensional IC technique with heart-cutting mode was developed to separate the ionic OPs from each other. On the first dimension, the OPs were pre-separated from the hexafluorophosphate anion, then the analytes were retarded on a preconcentration column and separated isocratically on the second dimension. Different stationary phases and eluents were used on the second dimension as compared to the first dimension [46]. The fluorinated decomposition product (8) with the m/z ratio of 266.9833 was formed by reaction of two OPs. Relating to this, Matsumoto et al. reported the polymerization of trimethylphosphate in LIB electrolytes [52]. However, the structure of the decomposition products formed by two OPs should be cleared by further structural clarification methods like nuclear magnetic resonance (NMR).

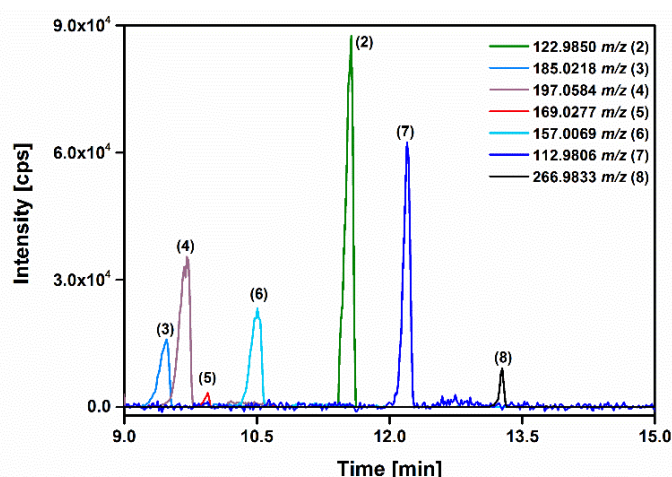


Figure 5. Electropherogram of the organophosphates (OPs) in the aged electrolyte sample containing dimethyl phosphate (DMP) and 1,3-propane sultone (PS).

In Figure 6, the electropherogram of the determined m/z ratios from the mixture of the LIB electrolyte, PS and DEP (9) is illustrated. Beside DEP (9), the decomposition products (2–7) were the same as in the previous sample. Additionally, the m/z ratio of 126.9966 (10) was

detected in this sample. This decomposition product was related to 2-((fluoro(2-(phosphonooxy)ethoxy)phosphoryl)oxy)ethanolate.

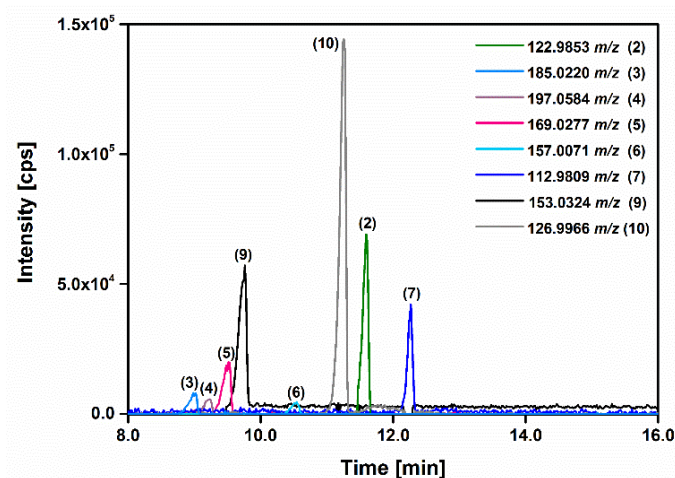


Figure 6. Electropherogram of the OPs in the aged electrolyte sample containing DEP (9) and PS.

The electropherogram in Figure 7 shows the detected m/z ratios of the aged electrolyte sample mixed with TEP and PS. Since DEP (10) was detected, it can be concluded that the compound was formed from TEP. Furthermore, the formation of DEP from TEP could be the reason that the same compounds were detected like in the electrolyte sample mixed with DEP and PS.

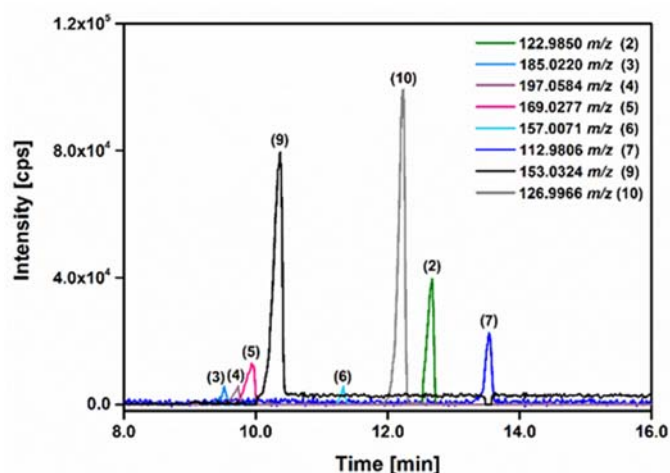


Figure 7. Electropherogram of the OPs in the aged electrolyte sample containing TEP and PS.

4. Conclusions

In this work, the optimization of a method for the hyphenation of a CE with Q-TOF-MS to detect anions in ILs and in LIB electrolytes was shown. For the detection of the anions, the buffer concentration, pH-value and CE conditions were optimized. The best buffer contained of 10 mM ammonium acetate with a pH-value of 10.3. The measurements were done at 25 °C, and a capillary voltage of 30.0 V was applied. The decomposition of the anions was investigated at room temperature and at 60 °C. The method for the detection of the TFSI[−] and FSI[−] anions showed short migration times and the reported results were confirmed by IC/ESI-MS [29]. The TFSI[−] and FSI[−] anions did not decompose at higher temperatures. The deviations of the detected m/z ratios of the anions to the calculated m/z ratios were lower than 3.0 ppm. Additionally, the developed method was applied to detect OPs in LIB electrolyte. In the reference sample,

only one decomposition product was detected. However, in the samples with the addition of DMP, DEP or TEP, more decomposition products were determined. In the sample with DMP, DMP reacted completely to other decomposition products, which included a long-chain OP not previously detected. In the DEP mixture with PS in the electrolyte, one more OP was formed compared to the use of DMP in the electrolyte mixture. The long-chain OP was not determined in this sample. The mixture of TEP, PS, and the LIB electrolyte showed the same OPs as in the DEP in the electrolyte mixture, since DEP was formed from TEP in this case. In the related electropherograms, the decomposition products were baseline-separated, although the structure of the OPs were fairly similar. The deviations of the detected m/z ratios of the OPs to the calculated m/z ratios were approx. 3.0 ppm. The hyphenation of the CE with the Q-TOF-MS is very suitable to investigate the formation of OPs in LIB electrolytes, since the baseline separation of OPs is possible without using a complex two-dimensional IC setup.

Author Contributions: M.P. and S.N. conceived and designed the experiments; M.P. performed the experiments and analyzed the data; M.P., M.W. and S.N. wrote the paper.

Conflicts of Interest: The authors declare no conflict of interest.

References

- Poole, C.F.; Lenca, N. Green sample-preparation methods using room-temperature ionic liquids for the chromatographic analysis of organic compounds. *TrAC Trends Anal. Chem.* **2015**, *71*, 144–156. [\[CrossRef\]](#)
- Fernicola, A.; Scrosati, B.; Ohno, H. Potentialities of ionic liquids as new electrolyte media in advanced electrochemical devices. *Ionics* **2006**, *12*, 95–102. [\[CrossRef\]](#)
- Keil, P.; Kick, M.; König, A. Long-term stability, regeneration and recycling of imidazolium-based ionic liquids. *Chem. Ing. Tech.* **2012**, *84*, 859–866. [\[CrossRef\]](#)
- Crowhurst, L.; Mawdsley, P.R.; Perez-Arlandis, J.M.; Salter, P.A.; Welton, T. Solvent-solute interactions in ionic liquids. *Phys. Chem. Chem. Phys.* **2003**, *5*, 2790–2794. [\[CrossRef\]](#)
- Rupp, B.; Schmuck, M.; Balducci, A.; Winter, M.; Kern, W. Polymer electrolyte for lithium batteries based on photochemically crosslinked poly(ethylene oxide) and ionic liquid. *Eur. Polym. J.* **2008**, *44*, 2986–2990. [\[CrossRef\]](#)
- Amereller, M.; Schedlbauer, T.; Moosbauer, D.; Schreiner, C.; Stock, C.; Wudy, F.; Zugmann, S.; Hammer, H.; Maurer, A.; Gschwind, R.M.; et al. Electrolytes for lithium and lithium ion batteries: From synthesis of novel lithium borates and ionic liquids to development of novel measurement methods. *Prog. Solid State Chem.* **2014**, *42*, 39–56. [\[CrossRef\]](#)
- Diallo, A.-O.; Morgan, A.B.; Len, C.; Marlair, G. An innovative experimental approach aiming to understand and quantify the actual fire hazards of ionic liquids. *Energy Environ. Sci.* **2013**, *6*, 699–710. [\[CrossRef\]](#)
- Garcia, B.; Lavallée, S.; Perron, G.; Michot, C.; Armand, M. Room temperature molten salts as lithium battery electrolyte. *Electrochim. Acta* **2004**, *49*, 4583–4588. [\[CrossRef\]](#)
- Peng, C.; Yang, L.; Zhang, Z.; Tachibana, K.; Yang, Y. Anodic behavior of Al current collector in 1-alkyl-3-methylimidazolium bis[(trifluoromethyl)sulfonyl] amide ionic liquid electrolytes. *J. Power Sources* **2007**, *173*, 510–517. [\[CrossRef\]](#)
- Cho, E.; Mun, J.; Chae, O.B.; Kwon, O.M.; Kim, H.-T.; Ryu, J.H.; Kim, Y.G.; Oh, S.M. Corrosion/passivation of aluminum current collector in bis(fluorosulfonyl)imide-based ionic liquid for lithium-ion batteries. *Electrochem. Commun.* **2012**, *22*, 1–3. [\[CrossRef\]](#)
- Krämer, E.; Schedlbauer, T.; Hoffmann, B.; Terborg, L.; Nowak, S.; Gores, H.J.; Passerini, S.; Winter, M. Mechanism of anodic dissolution of the aluminum current collector in 1 M LiTFSI EC:DEC 3:7 in rechargeable lithium batteries. *J. Electrochem. Soc.* **2013**, *160*, A356–A360. [\[CrossRef\]](#)
- Krämer, E.; Passerini, S.; Winter, M. Dependency of aluminum collector corrosion in lithium ion batteries on the electrolyte solvent. *ECS Electrochem. Lett.* **2012**, *1*, C9–C11. [\[CrossRef\]](#)
- Baranyai, K.J.; Deacon, G.B.; MacFarlane, D.R.; Pringle, J.M.; Scott, J.L. Thermal degradation of ionic liquids at elevated temperatures. *Aust. J. Chem.* **2004**, *57*, 145–147. [\[CrossRef\]](#)
- Liang, R.; Yang, M.; Xuan, X. Thermal stability and thermal decomposition kinetics of 1-butyl-3-methylimidazolium dicyanamide. *Chin. J. Chem. Eng.* **2010**, *18*, 736–741. [\[CrossRef\]](#)
- Kamavaram, V.; Reddy, R.G. Thermal stabilities of di-alkylimidazolium chloride ionic liquids. *Int. J. Therm. Sci.* **2008**, *47*, 773–777. [\[CrossRef\]](#)

16. Fox, D.M.; Gilman, J.W.; De Long, H.C.; Trulove, P.C. TGA decomposition kinetics of 1-butyl-2,3-dimethylimidazolium tetrafluoroborate and the thermal effects of contaminants. *J. Chem. Thermodyn.* **2005**, *37*, 900–905. [[CrossRef](#)]
17. Arellano, I.H.J.; Guarino, J.G.; Paredes, F.U.; Arco, S.D. Thermal stability and moisture uptake of 1-alkyl-3-methylimidazolium bromide. *J. Therm. Anal. Calorim.* **2011**, *103*, 725–730. [[CrossRef](#)]
18. Kosmulski, M.; Gustafsson, J.; Rosenholm, J.B. Thermal stability of low temperature ionic liquids revisited. *Thermochim. Acta* **2004**, *412*, 47–53. [[CrossRef](#)]
19. Valkenburg, M.E.V.; Vaughn, R.L.; Williams, M.; Wilkes, J.S. Thermochemistry of ionic liquid heat-transfer fluids. *Thermochim. Acta* **2005**, *425*, 181–188. [[CrossRef](#)]
20. Chambreau, S.D.; Boatz, J.A.; Vaghjiani, G.L.; Koh, C.; Kostko, O.; Golan, A.; Leone, S.R. Thermal decomposition mechanism of 1-ethyl-3-methylimidazolium bromide ionic liquid. *J. Phys. Chem. A* **2011**, *116*, 5867–5876. [[CrossRef](#)] [[PubMed](#)]
21. Chancelier, L.; Diallo, A.O.; Santini, C.C.; Marlair, G.; Gutel, T.; Mailley, S.; Len, C. Targeting adequate thermal stability and fire safety in selecting ionic liquid-based electrolytes for energy storage. *Phys. Chem. Chem. Phys.* **2014**, *16*, 1967–1976. [[CrossRef](#)] [[PubMed](#)]
22. Yuan, L.; Xu, C.; Peng, J.; Xu, L.; Zhai, M.; Li, J.; Wei, G.; Shen, X. Identification of the radiolytic product of hydrophobic ionic liquid [C₄mim][NTf₂] during removal of Sr²⁺ from aqueous solution. *Dalton Trans.* **2009**, *14*, 7873–7875. [[CrossRef](#)] [[PubMed](#)]
23. Earle, M.J.; Gordon, C.M.; Plechkova, N.V.; Seddon, K.R.; Welton, T. Decolorization of ionic liquids for spectroscopy. *Anal. Chem.* **2007**, *79*, 758–764. [[CrossRef](#)] [[PubMed](#)]
24. Meine, N.; Benedito, F.; Rinaldi, R. Thermal stability of ionic liquids assessed by potentiometric titration. *Green Chem.* **2010**, *12*, 1711–1714. [[CrossRef](#)]
25. Abdul-Sada, A.K.; Greenway, A.M.; Seddon, K.R.; Welton, T. A fast atom bombardment mass spectrometric study of room-temperature 1-ethyl-3-methylimidazolium chloroaluminate(iii) ionic liquids. Evidence for the existence of the decachlorotrialuminate(iii) anion. *Organ. Mass Spectrom.* **1993**, *28*, 759–765. [[CrossRef](#)]
26. Nockemann, P.; Binnemans, K.; Driesen, K. Purification of imidazolium ionic liquids for spectroscopic applications. *Chem. Phys. Lett.* **2005**, *415*, 131–136. [[CrossRef](#)]
27. Hao, F.; Haddad, P.R.; Ruther, T. ICdetermination of halide impurities in ionic liquids. *Chromatographia* **2008**, *67*, 495–498. [[CrossRef](#)]
28. Villagrán, C.; Deetlefs, M.; Pitner, W.R.; Hardacre, C. Quantification of halide in ionic liquids using ion chromatography. *Anal. Chem.* **2004**, *76*, 2118–2123. [[CrossRef](#)] [[PubMed](#)]
29. Pyschik, M.; Winter, M.; Nowak, S. Determination and quantification of cations in ionic liquids by capillary electrophoresis-mass spectrometry. *J. Chromatogr. A* **2017**, *1485*, 131–141. [[CrossRef](#)] [[PubMed](#)]
30. Pyschik, M.; Schultz, C.; Passerini, S.; Winter, M.; Nowak, S. Aging of cations of ionic liquids monitored by ion chromatography hyphenated to an electrospray ionization mass spectrometer. *Electrochim. Acta* **2015**, *176*, 1143–1152. [[CrossRef](#)]
31. Pyschik, M.; Kraft, V.; Passerini, S.; Winter, M.; Nowak, S. Thermal aging of anions in ionic liquids containing lithium salts by IC/ESI-MS. *Electrochim. Acta* **2014**, *130*, 426–430. [[CrossRef](#)]
32. Pyschik, M.; Klein-Hitpaß, M.; Girod, S.; Winter, M.; Nowak, S. Capillary electrophoresis with contactless conductivity detection for the quantification of fluoride in lithium ion battery electrolytes and in ionic liquids—a comparison to the results gained with a fluoride ion-selective electrode. *Electrophoresis* **2017**, *38*, 533–539. [[CrossRef](#)] [[PubMed](#)]
33. Schmitz, R.W.; Murmann, P.; Schmitz, R.; Müller, R.; Krämer, L.; Kasnatscheew, J.; Isken, P.; Niehoff, P.; Nowak, S.; Rösenthaller, G.-V.; et al. Investigations on novel electrolytes, solvents and SEI additives for use in lithium-ion batteries: Systematic electrochemical characterization and detailed analysis by spectroscopic methods. *Prog. Solid State Chem.* **2014**, *42*, 65–84. [[CrossRef](#)]
34. Zinigrad, E.; Larush-Asraf, L.; Gnanaraj, J.S.; Sprecher, M.; Aurbach, D. On the thermal stability of LiPF₆. *Thermochim. Acta* **2005**, *438*, 184–191. [[CrossRef](#)]
35. Campion, C.L.; Li, W.; Lucht, B.L. Thermal decomposition of LiPF₆-based electrolytes for lithium-ion batteries. *J. Electrochem. Soc.* **2005**, *152*, A2327–A2334. [[CrossRef](#)]
36. Handel, P.; Fauler, G.; Kapper, K.; Schmuck, M.; Stangl, C.; Fischer, R.; Uhlig, F.; Koller, S. Thermal aging of electrolytes used in lithium-ion batteries—an investigation of the impact of protic impurities and different housing materials. *J. Power Sources* **2014**, *267*, 255–259. [[CrossRef](#)]

37. Kraft, V.; Grützke, M.; Weber, W.; Winter, M.; Nowak, S. Ion chromatography electrospray ionization mass spectrometry method development and investigation of lithium hexafluorophosphate-based organic electrolytes and their thermal decomposition products. *J. Chromatogr. A* **2014**, *1354*, 92–100. [[CrossRef](#)] [[PubMed](#)]
38. Terborg, L.; Nowak, S.; Passerini, S.; Winter, M.; Karst, U.; Haddad, P.R.; Nesterenko, P.N. Ion chromatographic determination of hydrolysis products of hexafluorophosphate salts in aqueous solution. *Anal. Chim. Acta* **2012**, *714*, 121–126. [[CrossRef](#)] [[PubMed](#)]
39. Campion, C.L.; Li, W.; Euler, W.B.; Lucht, B.L.; Ravdel, B.; DiCarlo, J.F.; Gitzendanner, R.; Abraham, K.M. Suppression of toxic compounds produced in the decomposition of lithium-ion battery electrolytes. *Electrochem. Solid-State Lett.* **2004**, *7*, A194–A197. [[CrossRef](#)]
40. Vetter, J.; Novák, P.; Wagner, M.R.; Veit, C.; Möller, K.C.; Besenhard, J.O.; Winter, M.; Wohlfahrt-Mehrens, M.; Vogler, C.; Hammouche, A. Ageing mechanisms in lithium-ion batteries. *J. Power Sources* **2005**, *147*, 269–281. [[CrossRef](#)]
41. Weber, W.; Wagner, R.; Streipert, B.; Kraft, V.; Winter, M.; Nowak, S. Ion and gas chromatography mass spectrometry investigations of organophosphates in lithium ion battery electrolytes by electrochemical aging at elevated cathode potentials. *J. Power Sources* **2016**, *306*, 193–199. [[CrossRef](#)]
42. Vortmann, B.; Nowak, S.; Engelhard, C. Rapid characterization of lithium ion battery electrolytes and thermal aging products by low-temperature plasma ambient ionization high-resolution mass spectrometry. *Anal. Chem.* **2013**, *85*, 3433–3438. [[CrossRef](#)] [[PubMed](#)]
43. Weber, W.; Kraft, V.; Grützke, M.; Wagner, R.; Winter, M.; Nowak, S. Identification of alkylated phosphates by gas chromatography–mass spectrometric investigations with different ionization principles of a thermally aged commercial lithium ion battery electrolyte. *J. Chromatogr. A* **2015**, *1394*, 128–136. [[CrossRef](#)] [[PubMed](#)]
44. Kraft, V.; Weber, W.; Streipert, B.; Wagner, R.; Schultz, C.; Winter, M.; Nowak, S. Qualitative and quantitative investigation of organophosphates in an electrochemically and thermally treated lithium hexafluorophosphate-based lithium ion battery electrolyte by a developed liquid chromatography-tandem quadrupole mass spectrometry method. *RSC Adv.* **2016**, *6*, 8–17. [[CrossRef](#)]
45. Kraft, V.; Weber, W.; Grützke, M.; Winter, M.; Nowak, S. Study of decomposition products by gas chromatography-mass spectrometry and ion chromatography-electrospray ionization-mass spectrometry in thermally decomposed lithium hexafluorophosphate-based lithium ion battery electrolytes. *RSC Adv.* **2015**, *5*, 80150–80157. [[CrossRef](#)]
46. Kraft, V.; Grützke, M.; Weber, W.; Menzel, J.; Wiemers-Meyer, S.; Winter, M.; Nowak, S. Two-dimensional ion chromatography for the separation of ionic organophosphates generated in thermally decomposed lithium hexafluorophosphate-based lithium ion battery electrolytes. *J. Chromatogr. A* **2015**, *1409*, 201–209. [[CrossRef](#)] [[PubMed](#)]
47. Grützke, M.; Kraft, V.; Hoffmann, B.; Klamor, S.; Diekmann, J.; Kwade, A.; Winter, M.; Nowak, S. Aging investigations of a lithium-ion battery electrolyte from a field-tested hybrid electric vehicle. *J. Power Sources* **2015**, *273*, 83–88. [[CrossRef](#)]
48. Terborg, L.; Weber, S.; Passerini, S.; Winter, M.; Karst, U.; Nowak, S. Development of gas chromatographic methods for the analyses of organic carbonate-based electrolytes. *J. Power Sources* **2014**, *245*, 836–840. [[CrossRef](#)]
49. Terborg, L.; Weber, S.; Blaske, F.; Passerini, S.; Winter, M.; Karst, U.; Nowak, S. Investigation of thermal aging and hydrolysis mechanisms in commercial lithium ion battery electrolyte. *J. Power Sources* **2013**, *242*, 832–837. [[CrossRef](#)]
50. Appetecchi, G.B.; Scaccia, S.; Tizzani, C.; Alessandrini, F.; Passerini, S. Synthesis of hydrophobic ionic liquids for electrochemical applications. *J. Electrochem. Soc.* **2006**, *153*, A1685–A1691. [[CrossRef](#)]
51. Mönnighoff, X.; Murmann, P.; Weber, W.; Winter, M.; Nowak, S. Post-mortem investigations of fluorinated flame retardants for lithium ion battery electrolytes by gas chromatography with chemical ionization. *Electrochim. Acta* **2017**, *246*, 1042–1051. [[CrossRef](#)]
52. Matsumoto, K.; Martinez, M.; Gutel, T.; Mailley, S.; De vito, E.; Patoux, S.; Inoue, K.; Utsugi, K. Stability of trimethyl phosphate non-flammable based electrolyte on the high voltage cathode (LiNi_{0.5}Mn_{1.5}O₄). *J. Power Sources* **2015**, *273*, 1084–1088. [[CrossRef](#)]

